A Section 508–conformant HTML version of this article is available at https://doi.org/10.1289/EHP11495.

Quantitative Microbial Risk Assessment of Contracting COVID-19 Derived from Measured and Simulated Aerosol Particle Transmission in Aircraft Cabins

Jack F. Schijven,[1,2] Theo van Veen,[3] Christiaan Delmaar,[1] Johan Kos,[3] Lucie Vermeulen,[1] Rui Roosien,[3] Frank Verhoeven,[4] Maarten Schipper,[1] Bram Peerlings,[3] Erwin Duizer,[1] Jonathan Derei,[3] Wim Lammen,[3] Onno Bartels,[3] Harmen van der Ven,[3] Robert Maas,[3] and Ana Maria de Roda Husman[1,5]

[1]Centre for Infectious Disease Control, National Institute for Public Health and the Environment, Bilthoven, the Netherlands
[2]Department of Earth Sciences, Utrecht University, Utrecht, the Netherlands
[3]Royal Netherlands Aerospace Centre, Amsterdam, the Netherlands
[4]Medspray, Enschede, the Netherlands
[5]Institute for Risk Assessment Sciences, Utrecht University, Utrecht, the Netherlands

Background: SARS-CoV-2 can be effectively transmitted between individuals located in close proximity to each other for extended durations. Aircraft provide such conditions. Although high attack rates during flights were reported, little was known about the risk levels of aerosol transmission of SARS-CoV-2 in aircraft cabins.

Objectives: The major objective was to estimate the risk of contracting COVID-19 from transmission of aerosol particles in aircraft cabins.

Methods: In two single-aisle and one twin-aisle aircraft, dispersion of generated aerosol particles over a seven-row economy class cabin section was measured under cruise and taxi conditions and simulated with a computational fluid dynamic model under cruise conditions. Using the aerosol particle dispersion data, a quantitative microbial risk assessment was conducted for scenarios with an asymptomatic infectious person expelling aerosol particles by breathing and speaking. Effects of flight conditions were evaluated using generalized additive mixed models.

Results: Aerosol particle concentration decreased with increasing distance from the infectious person, and this decrease varied with direction. On a typical flight with an average shedder, estimated mean risk of contracting COVID-19 ranged from 1.3×10^{-3} to 9.0×10^{-2}. Risk increased to 7.7×10^{-2} with a super shedder (<3% of cases) on a long flight. Risks increased with increasing flight duration: 2–23 cruise flights of typical duration and 2–10 flights of longer duration resulted in at least 1 case of COVID-19 due to onboard aerosol transmission by one average shedder, and in the case of one super shedder, at least 1 case in 1–3 flights of typical duration cruise and 1 flight of longer duration.

Discussion: Our findings indicate that the risk of contracting COVID-19 by aerosol transmission in an aircraft cabin is low, but it will not be zero. Testing before boarding may help reduce the chance of a (super)shedder boarding an aircraft and mask use further reduces aerosol transmission in the aircraft cabin. https://doi.org/10.1289/EHP11495

Introduction

SARS-CoV-2 spreads via respiratory droplets, including aerosol particles.[1] To limit the fast global spread of the disease, international aviation was brought to a standstill in March 2020. After the aviation sector introduced measures to prevent the spread of the disease, aviation slowly resumed in June 2020. At that time, little was known about the transmission of SARS-CoV-2 in aircraft cabins.

Early on in the pandemic, before preventive measures were taken, air travel was found to be contributing to the spread of COVID-19 outside of China.[2,3] As described for other pandemic viruses such as influenza A/H1N1 2009 and SARS-CoV,[4,5] in-flight transmission of SARS-CoV-2 has been reported.[6–9] In their systematic review, Rosca et al.[10] identified 130 unique flights where 273 index cases led to 64 reported secondary cases, with an attack rate ranging from 0% to 8.2% in studies where >80% of the passengers and crew were followed-up. Rosca et al.[10] noted that a major limitation of many studies was the possibility of asymptomatic secondary cases not being investigated, lowering the quality of case ascertainment. Toyokawa et al.[11] found that risk factors for on board transmission were not using or partially using a face mask, as well as seating within two rows from the index passenger. Other studies also observed that attack rates were higher with closer seating proximity to a symptomatic index passenger.[7] Moreover, asymptomatic transmission may also occur[12] even under strict infection control procedures, such as mask use.[13] An elevated risk was indicated for passengers in window seats.[8] Rosca et al.[10] stated that it is clear that SARS-CoV-2 transmission aboard aircraft can occur, but that the published epidemiological data did not permit any conclusive assessment of likelihood and extent.

These epidemiological studies provided insights into the transmission dynamics of the infection and effective outbreak control measures. However, real-time analyses can be challenging owing to the incubation period, turnaround times required for testing, and multiple exposures occurring through varying transmission routes. Alternative study approaches encompass modeling such as quantitative microbial risk assessment (QMRA).[14] QMRA has been applied for SARS-CoV-2 exposure via droplets and aerosol particles from, for example, wastewater treatment plants and indoor drainage systems.[15] QMRA has been applied in an aircraft setting for the airborne disease tuberculosis,[16] but not yet for SARS-CoV-2, to our knowledge.

This study aimed to assess the risk of contracting COVID-19 via aerosol transmission of SARS-CoV-2 in aircraft cabins. Dispersion of aerosol particles under real transport conditions was determined from measurements in experiments and from data generated by computational fluid dynamics (CFD) simulations. Using the dispersion information, risk of contracting COVID-19 was estimated in scenarios with one contagious asymptomatic passenger (index) exposing other passengers to aerosol particles containing SARS-CoV-2 that were emitted via breathing and speaking, with or without a face mask, using QMRA. The combination of data from measurements and CFD simulations provide an integral method to estimate the realistic risk of contracting COVID-19

Address correspondence to Jack F. Schijven. Email: jack.schijven@rivm.nl.
Supplemental Material is available online (https://doi.org/10.1289/EHP11495).
The authors declare they have no actual or potential competing financial interests.
Received 27 April 2022; Revised 13 July 2023; Accepted 13 July 2023; Published 17 August 2023.
Note to readers with disabilities: *EHP* strives to ensure that all journal content is accessible to all readers. However, some figures and Supplemental Material published in *EHP* articles may not conform to 508 standards due to the complexity of the information being presented. If you need assistance accessing journal content, please contact ehpsubmissions@niehs.nih.gov. Our staff will work with you to assess and meet your accessibility needs within 3 working days.

during aircraft transport. A description of methodology and a discussion of the results aimed at the general public was published by the Royal Netherlands Aerospace Centre (Royal NLR) and the National Institute for Public Health and the Environment (RIVM).[17] This article provides a more detailed presentation of the work aimed at the scientific community.

Methods

General Study Design

The overall goal of this study was to estimate the risk of contracting COVID-19 using measured and CFD simulations of aerosol particles to model transmitted SARS-CoV-2 viral particles from a single asymptomatic infectious passenger (index), in three types of common passenger aircraft. During the pandemic, persons with symptoms were expected to stay at home. However, an asymptomatic index passenger could be as infectious as a person with symptoms. After the pandemic, passengers with symptoms are allowed to board. Because an asymptomatic passenger is not expected to emit aerosol via coughing or sneezing, in this study we considered only emission via breathing and speaking. Data for the risk assessment were collected by means of measuring the dispersion of artificially generated aerosol particles in the aircraft cabin under a variety of cabin environmental conditions. As an independent verification of the plausibility of the measurement outcomes, dispersion of aerosol particles emitted by the index passenger was also simulated using a CFD model. The CFD model also allowed us to evaluate the sensitivity of the outcomes to changes in the index passenger location, which, in contrast to the measurements, could be varied in the simulations. Measured and CFD-simulated aerosol particle dispersion data was used as input for the QMRA. Cruise conditions were measured and simulated. Taxi conditions were measured but not simulated to save on computation time.

QMRA was conducted for discrete scenarios, generally assuming a full aircraft with passengers wearing a disposable face mask (over nose and mouth) for 90% of the flight time. Scenarios varied, among others, in assumptions on flight duration, taxi and cruise phases, and viral shedding of the index passenger. Boarding and deboarding phases in the aircraft and at the airport terminal and boarding bridges were not investigated. Other transmission routes (direct by droplets and touch, indirect via fomites) than the aerosol transmission route were not investigated.

Measurements

The measurement campaign consisted of 80 measurement runs inside the cabin of a Boeing 737-800 (single-aisle, capacity 185 passengers), Airbus A320 (single-aisle, capacity 180 passengers), and Boeing 787-9 (twin-aisle, capacity 280 passengers) aircraft. All aircraft were measured in taxi (stationary, main engines running, power setting representative for taxiing, auxiliary power unit off, doors closed) and cruise conditions (straight steady flight at cruise speed and altitude, normal operating conditions; for the B737, A320, and B787, cruise speeds relative to air were 410 km/h, 440 km/h, and 460 km/h respectively; and the altitude was 12 km for all aircraft). The aircraft were chartered from commercial operators. The operators facilitated a safe test flight but were not involved in the study design or risk assessment. Each measurement run tested a scenario specified by flight condition, pack setting, and gasper setting, as well as whether or not the index passenger was wearing a mask (Table 1). A gasper is an adjustable ventilation outlet in passenger transport aircraft. The gaspers are located in the passenger service unit above the passengers. Passengers may adjust the direction and the strength of the air flow by turning the revolving control.[18]

The test section included seven rows of the economy class cabin. Lifesize manikins were placed on the seats to mimic the presence of passengers. During taxi testing, electrically heated blankets covered the manikins to mimic the heat signature of human passengers. For safety reasons, the blankets had to be switched off during flight.

The index passenger was assumed to sit in a middle seat in the middle row of the test section, called the index location. This location was chosen to provide the best impression of directional effects. The manikin at the index location was coupled to an aerosol generator that was spreading a proxy of human saliva. In the single-aisle aircraft, the index passenger was positioned in seat E. In the twin-aisle aircraft the index passenger was positioned in seat E for most runs and, alternatively, in seats B or C for a few runs (Figure 1). One seat behind and to the left of the index passenger was used by the operator of the aerosol generator (customized Pulmospray; Medspray). The droplets were generated by a silicon nozzle chip (design 1513; Medspray) that contained 85 pores of 1.9 μm diameter and which used the Rayleigh jet breakup principle to create consistent droplets of known size and constant droplet generation.

At the seat of the index passenger, the nozzle was mounted on the head of the manikin. The nozzle was connected to a syringe (1-mL Luer-lok; BD) and a manually operated air pump (Dresco), combined with an airflow meter (TSI 4040), simulating the breathing of a human with multiple puffs of aerosol particles. As a proxy of human saliva, water with 1% wt/wt glycerol and 2% wt/wt sodium chloride was used to generate the aerosol particles.[19] The total excipient concentration (what remains after evaporation) was 3% wt/wt, in line with a volume reduction of 27 times by evaporation of aerosol particles from human saliva as reported by Liu et al.[20] The aerosol particle distribution was aimed to represent that of a breathing/speaking person (80/20 ratio[21,22]). A total of 700 μL of artificial saliva was dispersed in a time span of $\sim$3 min in each measurement run. The nozzle required pressurized air at a flow of 15 L/min

Table 1. Conditions in measurement runs.

Parameter	Single-aisle	Twin-aisle	Rationale
Phase of flight	Cruise, taxi	Cruise, taxi	Two phases of interest, owing to different ambient air pressure levels
Gasper settings	All closed, middle open, all open	Middle gaspers open	Possible (local) effect on dispersion, easy to manipulate
Mask on index passenger	Mask, no mask	Mask, no mask	Assess the effect of a face mask on particle dispersion in an aircraft
Heated blankets on manikins	On, off	On, off	Simulate heat coming from passengers. Only used during the taxi phase
Air conditioning (pack setting)	Normal, high	Normal	Possible (cabin) effect on dispersion
Index location	Seat E, row 24/25	Seats E, B, row 35	Effect of location index

Note: A single measurement run was conducted for each unique combination of experiment settings.

Figure 1. Measurement setup showing the seats of the seven rows with the manikins: (A) single-aisle, (B) twin-aisle, and (C) nozzle connected to aerosol generator at index passenger location. ©NLR & RIVM. Note: APS, Aerodynamic Particle Sizer; HPLC, high-performance liquid chromatography; PM, particulate matter.

at 2 kPa, representative of breathing. Losses due to residues adhering to the measurement setup were estimated at 11 µL, thus the total volume of dispersed liquid was 689 µL. After initial evaporation, the emitted aerosol particle volume, $V_{emission}$, was 25 µL. Depending on the scenario, the nozzle was either uncovered or covered by a nonmedical face mask (EN 14683 IIR), replicating the effect of a face mask on the index passenger.

Aerosol particle concentrations (number of particles per centimeter cubed) were logged with Sensirion Particulate Matter (PM) sensors (SPS30), placed on each manikin (Figure 1). In addition, two TSI Aerodynamic Particle Sizer (APS) 3321 sensors measured the size distribution at two seats. One APS sensor was placed right next to the source with the inhalation tube tilted toward the index passenger. The other APS sensor was placed two rows in front of the index passenger. Temperature and relative humidity were logged at the seats using EasyLog USB2 LCD + data loggers. Air flow direction and speed in three dimensions were measured at various locations in front of and behind the seven-row section using a Gill Windmaster Pro 3D anemometer.

For translation of the findings to the QMRA, it was assumed that the spread of experimental particles with an initial size of up to 20 µm was the same because in that size range convective transport dominates.[20] With the CFD simulations, particles up to 20.0 µm in diameter were replicated. The number of aerosol particles released in the cabin was larger than produced by average humans (~ 7 billion as estimated from the total volume that was emitted and their size distribution that was determined with an APS) to obtain reliable counts for determining the fractions used in the QMRA.

The measured particle number concentrations in air were divided over five different size classes: 0.3–0.5 µm, 0.5–1.0 µm, 1.0–2.5 µm, 2.5–4.0 µm, and 4.0–10.0 µm. Particle counts per centimeter cubed air were determined per diameter class, per second, for a period of 5–10 min after the start of the aerosol emission. The APS sensors had a native measurement range of 0.5–20.0 µm and were used to determine the size distribution of the particles. For the determination of the particle dispersion in number and sizes of the particles, measurements from both sensors were combined. The particles within the 0.5- and 2.5-µm range bins were used as a reference to deduce the total number of particles in the range 0.5–10 µm per run, per seat. The particle size distribution as determined in the laboratory and measured by an APS was used to determine the number of particles within the bin size per run and per seat. The PM sensor in the native measurement range 0.5–2.5 µm was compared with an optical particle sensor (TSI 3330) by the German Aerospace Centre (DLR) in a laboratory setting. The counts of particle size bins 0.3–1.0 µm and 1.0–2.5 µm, where found to be the same with a deviation of not more than 10%.

CFD Simulations

CFD simulations were carried out for the single-aisle Airbus A320 aircraft and the twin-aisle Boeing 787-9 aircraft that were used in the measurements. In the CFD simulations, the starting position of the cloud with spatially uniform distributed aerosol particles was modeled as a 10-cm diameter sphere located 10 cm in front of the index passenger. The particle size distribution at the starting position was defined by the two source definitions of breathing and speaking (80/20 ratio).[21,22] Complementing the measurements, the particle range was expanded to 20 µm in simulations.

The air flow in the aircraft cabin was simulated with the buoyant Boussinesq[23] solver of OpenFOAM,[24] and the dispersion of particles in this air flow was simulated with the Lagrangian

approach of the same reference, taking into account the cabin configuration of the aircraft types, cabin environmental conditions, and ventilation system properties. The surface temperature of the passengers at the seven-row section were modeled according to Tanabe et al.,[25] unmoving and in a seated and forward-looking position. The radiated heat of a seated passenger was assumed to be $130.5\,W/m^2$ for light activities. Seats were positioned in their upright position with tray-tables stowed away and all luggage was assumed to be stored in luggage bins. The seat of the index passenger was varied over the middle row of the seven-row section.

For the single-aisle aircraft, inflow of air was modeled through side, ceiling, and gasper inlets following manufacturer specifications that were provided by the aircraft operator (the actual specifications of the aircraft are not accessible for the general public). For the twin-aisle aircraft, inflow rates per inlet were selected so as to limit differences between measurement and simulation results. The inflow temperature was set so to maintain a constant cabin air temperature (measurements 19–24°C, simulations 22°C and 24°C). Based on measured temperatures with an infrared camera (FLIR E75) and temperature sensors, surfaces inside the cabin (seats, luggage bins, floor, and roof) were treated as adiabatic, whereas for the sidewalls, the temperatures were set to fixed values—as is common practice in this type of modelling[26,27]—varying between 17°C and 19°C.

The influence of air flow (in turn, influenced by, e.g., inflow and outflow and buoyancy effects owing to the cabin occupants emitting heat) and gravity on aerosol particle trajectories was modeled, whereas the possible influence of inhalation and exhalation by or movement of cabin occupants was not included. As simplifications, aerosol particles were conservatively modeled to bounce back rather than to stick to the surface upon impact, interactions between aerosol particles were not modeled, and the size of aerosol particles was modeled to remain fixed during their movement through the cabin. These aspects of the behavior of aerosol particles are an inherent part of the measurements, and the simplification of the CFD modeling may therefore give rise to slightly deviating outcomes.

In each simulation run, various quantities were logged to derive the input for the QMRA. These quantities were determined for inhalation boxes, defined as $30\times30\times30$-cm cubes, centered at the nose of other cabin occupants, based on Gupta et al.[26] The total volume of aerosol particles and the corresponding residence time, at a 1-s resolution, was exported as input for the QMRA, as well as the number and volume of aerosol particles per size (diameter) bin in each inhalation box.

Environmental conditions (temperature, relative humidity, air exchange rate, air flow direction) and other input parameters (dimensions) used for the simulations were matched to those observed during the measurements.[17] Simulated and counted numbers of aerosol particles were compared for the single- and twin-aisle aircraft under cruise conditions.

QMRA

In the QMRA, the inhaled dose of virus at each seat, $d_{virus}[seat]$ was calculated as follows:

$$d_{virus}[seat] = f_{evap} \times c_{sputum} \times f_{mask} \times frac[seat] \times q_{src} \times t_{exp}, \quad (1)$$

where $f_{evap} \times c_{sputum}$ is the concentration of virus in the aerosol particles (numbers divided by volume), that was derived from the concentration of virus in sputum (numbers divided by volume), by assuming that sputum-generated aerosol particles will shrink by an additional factor of $1/f_{evap}$ owing to evaporation,[20] within a few tenths of a second[26]; f_{mask} is the assumed total filtering efficiency of masks combined for inhalation and exhalation; $frac$[seat] is the fraction of aerosol volume released that would be inhaled by a passenger at a seat; q_{src} is the emission volume rate of aerosol particles by an index passenger; and t_{exp} is the exposure duration.

The transform fraction $frac$ was determined in the measurements and CFD simulations for all seats in the cabin section by integrating the inhaled aerosol volume concentration c_V at a seat over the entire measurement or simulation run duration t_{run} and dividing by the total aerosol volume released $V_{emission}$:

$$frac = q_i \times \frac{1}{V_{emission}} \int_0^{t_{run}} c_V(t')dt' = q_i \times \frac{1}{V_{emission}} \times t_{run} \times c_{vol}, \quad (2)$$

where q_i is the inhalation rate of an exposed person at seat (equal to q_{src}) and c_{vol} is defined as the average of c_v over the experimental run duration. See Table 2 for all parameter values.

Calculation of risk. From the inhaled virus dose d_{virus}, risk of contracting COVID-19, P_{ill}, was calculated as a probability of that person contracting COVID-19:

$$P_{ill} = 1 - \exp\left(-frd_{virus}\right), \quad (3)$$

where f is the fraction of plaque forming units in virus RNA copies, and r is a dose–response parameter. Following Schijven et al.[29] f was set to 1.25×10^{-2}, and r to 5.6×10^{-2} (Table 2).

Because of a lack of dose–response data, the recommendation of Haas[30] to use the dose–response data for human coronavirus 229E as representative for SARS-CoV-2 was followed as a precautionary approach. These data encompass dose values and number of persons demonstrating symptoms. It was assumed that this dose–response relation for the risk of illness to exposure to 229E applied to SARS-CoV-2 as well. The combination of f and r corresponded to 6.9×10^{-4} virus RNA copies on average leading to contracting COVID-19 matched the number of viral genomes needed to initiate an infection of $\sim$1,000 (1–5,000) as based on a transmission network with 39 transmission events.[31]

The expected number of cases in the seven-row section was calculated by multiplying the mean risk with the number of passengers seated in the seven-row section and was assumed to be equal to the expected number of cases of contracting COVID-19 in the entire aircraft. The virus *dose* depends linearly on c_{sputum}, $fmask$, $frac$, q_{src}, and t_{exp} (Equation 1). If risk levels are low, risk may also be regarded as linearly dependent on these variables. Hence, a straightforward sensitivity analysis was conducted: by simply comparing the relative ranges these variables span. All computations of risk were conducted using Mathematica (version 12.3.1).[32]

Scenarios. Risk estimates were made for each seat in a set of seven rows around the index passenger. Risk outside this area was assumed to be negligible, as was justified by additional very low measurements outside the seven rows (within the same order of magnitude as the uncertainty margin of the PM sensors used). Input parameters were either fixed to a deterministic value representing a scenario assumption, or represented by a probability distribution to account for variability in the parameter value. Risk in each scenario was evaluated using Monte Carlo simulation in which 10,000 samples were taken from the probability distributions, resulting in a distribution of risk estimates per seat. Parameter values for c_{sputum} and q_{src} were as described by Schijven et al.[29] c_{sputum} was normally distributed on a $\log_{10}$-scale with a mean of 7.53 and standard deviation of 1.28.[29]

Table 2. Model parameters (Equations 1–3).

Model parameter	Value	Dimension	Reference
f_{evap}	27	—	Liu et al.[20]
c_{sputum}	10^Normal (7.52, 1.28)	RNA copies/mL	Schijven et al.[29]
f_{mask}	0.7	—	Chu et al.[33]; Esposito et al.[34]; Fisher et al.[35]; Howard et al.[36]; Leung et al.[37]; Cheng et al.[38]
q_{src}	10^Normal $(\log_{10}(6.8), 0.05)$	L/min	Colbeck[19]
t_{exp}	Scenario dependent	—	—
f	1.3×10^{-2}	—	Schijven et al.[29]
r	5.6×10^{-2}	—	Haas et al.[30]

Note: —, not applicable.

The filter efficiency of masks is reported to be highly variable, ranging from ∼30% to >90%.[33–38] In the present study, it was assumed that inhalation filtering (removal) efficiency was 30% and that the reduction in droplet and aerosol emissions was 60% when masks are worn. This yielded a total risk reduction of ∼70%, in accordance with the face mask efficacy derived by Cheng et al.[38]

Scenarios were constructed by varying cruise flight duration (typical or long), the viral load of the index passenger [based on population data or a passenger who sheds an extraordinary amount of infectious aerosol particles (a super shedder)], and flight conditions (cruise or taxiing). For mask wearing, an assumption was made that masks are worn during flight except for a period in which meals or snacks are served.

For flight duration, typical and long flight durations were adopted based the flights to and from Amsterdam Airport Schiphol in 2019. Typical cruise flight duration was 0.9 h and 1.4 h for the two single-aisle aircraft, and 8.7 h for the twin-aisle aircraft. The long (95th percentile) cruise flight duration was 2.5 h and 3.6 h for the two single-aisle aircraft, and 11.1 h for the twin-aisle aircraft.

The typical duration that masks are not worn (owing to consumption of drinks, snacks, and meals on board) was estimated to be 10% of the total flight duration. Also included was the scenario in which masks were assumed not to be worn at all.

Virus shedding of the index passenger was based on data on q_{src} and c_{sputum}. In addition to the variable emission data described above, a deterministic super shedder scenario was included. A super shedder was defined as a person with a sputum viral load of 10^{10} RNA copies per milliliter (97.3% of virus concentrations is less than this value; Table 2).

Statistical Analysis of the Measurements

Estimated mean risks P_{ill} after 1 h of exposure per exposed passenger (manikin) and per run based on the measurements were subjected to statistical analysis as the dependent variable in R (version 3.6.0; R Development Core Team) for analyzing the effects of a number of variables. Values of p_{ill} equal to zero were excluded, because in those cases no PM sensor data were available. In the statistical analysis, mean p_{ill} values were $\log_{10}$ transformed.

Generalized additive mixed models (GAMMs) were fitted using package *gamm4* (version 0.2-6).[39] As fixed categorical effects, *aircraft* (single and two aisle), *gc* (taxi/cruise), *mask* (Yes/No), *heating* (Yes/No; only during taxi conditions), *gasper* (closed/open; affects air flow, only during taxi conditions) were entered into the models. *distance*, *oc* (cabin air temperature), and *rh* (relative humidity) were modeled with smooth additive effects, whereas *angle* (0–360 degrees, relative to the index passenger, where 0 degrees was along a row to the right) was modeled with a cyclic spline. *Run* was entered as a random intercept in the GAMM. GAMMs were fitted with restricted maximum likelihood. Significance and *p*-values were based on *t*-tests used the Satterthwaite method. An effect of *blankets* was not investigated because this effect could not be distinguished from *heating*. Similarly, an effect of *pack* was not investigated because this effect could not be distinguished from *gasper*. In R, the GAMM model was formulated as follows:

$$\log_{10}(P_{ill}) \sim \text{mask\_YN} + aircraft + gasper + heating +$$
$$s(oc, bs = \text{“ps”}, \text{k} = 4) +$$
$$s(rh, bs = \text{“ps”}, \text{k} = 4) +$$
$$s(dist, bs = \text{“ps”}, \text{k} = 5, \text{by} = aircraft) +$$
$$s(angle, bs = \text{“cc”}, \text{by} = aircraft),$$

where *s* is a function used in definition of smooth terms, with the parameter *bs* indicating the (penalized) smoothing basis to use (ps specifies P = splines and cc specifies acyclic cubic regression splines).

Results

All values of c_{Vol}, *frac*, and P_{ill} are listed in Excel Tables S1–S9.

Aerosol Particle Dispersion

After initial evaporation to the final size, the generated aerosol particles resembled aerosol particles exhaled by humans under typical breathing[21] and speaking conditions.[22] The generated particle diameters were in the range of 0.3–5.5 μm after evaporation of the solvent, whereas the initial wet size of the aerosol particle was three times larger. Aerosol emission by humans by speaking and breathing is known to include larger particles.[21,22]

Given the large number of inlets and outlets and fluctuations over time owing to changing conditions, air exchanges per hour were difficult to measure directly with the in-cabin measurements. Using the time between the instant the aerosol generator stopped emitting aerosol particles and the end of the measurement runs (3:42–8:12 min while on the ground, and 2:40–7:37 min during cruise) as indicative of the time until the cabin air is refreshed, the corresponding refresh rates varied between 7.3 and 22.5 air exchanges per hour.

Aerosol particle concentrations remained low for all seats in the measurement grid during the time between measurement runs. In addition, only very low numbers of aerosol particles were detected in the two rows in front of the measurement grids (within the same order of magnitude as the uncertainty margin of the PM sensors used). The values of the transfer fraction *frac* (Equation 2), virus dose, and associated risk values were highest next to the index position: in orders of magnitude of 10^{-4} to 10^{-3} for *frac*, 10^{1} to 10^{2} for virus dose, and 10^{-2} to 10^{-1} for the risks. All quantities declined by approximately one order of magnitude for the other seats within the seven rows. This general pattern was observed for all aircraft and measurement runs. For detailed samples of the transfer fractions of aerosol particles per seat for different measurement runs and aircraft, see Figures S1–S3 and Excel Tables S7–S9.

On average, the CFD simulations predicted 50% (single-aisle) or 70% (twin-aisle) more particles per seat than were found in the measurements (Tables S1 and S2). This may be explained by the

Table 3. Categorical fixed effects on the base-10 logarithm of the risk of contracting COVID-19 ($\log_{10}P_{ill}$).

Term	Estimate $\log_{10}P_{ill}$	Standard error $\log_{10}P_{ill}$	p-Value[a]	Mean effect on risk P_{ill}
All measurements without considering effects of gasper and heating				
Mask yes[b]	−0.57	0.014	$<2\times10^{-16}$	3.7 times lower
Twin-aisle aircraft[c]	0.51	0.019	$<2\times10^{-16}$	3.2 times higher
Taxi[d]	−1.6	0.15	$<2\times10^{-16}$	40 times lower
Twin-aisle aircraft × taxi[e]	−0.072	0.028	0.01	1.2 times lower
Measurements at taxi conditions considering effects of gasper and heating				
Mask_yes[b]	−0.58	0.014	$<2\times10^{-16}$	3.8 times lower
Twin-aisle aircraft[c]	0.39	0.019	$<2\times10^{-16}$	2.5 times higher
Gasper open[f]	0.17	0.020	$<2\times10^{-16}$	1.5 times higher
Heating on[g]	−0.24	0.027	$<2\times10^{-16}$	1.7 times lower

[a]GAMM[40] in R (version 3.6.0; R Development Core Team).
[b]Relative to mask no.
[c]Relative to single-aisle aircraft.
[d]Relative to flight.
[e]Interaction term.
[f]Relative to gasper closed.
[g]Relative to heating off.

conservative choice to simulate aerosol particles bouncing back from surfaces rather than sticking to surfaces.

Statistical Modeling and Analysis of the Measurements (Excel Tables S7–S9)

Table 3 summarizes the categorical effects on $\log_{10}P_{ill}$. The antilog of each of the coefficients given in Table 3 represents the factor by which the risk, P_{ill}, changes, which is the effect of a condition. The adjusted R^2 of the GAMM model was 73%. Figure 2 depicts box plots of $\log_{10}P_{ill}$ according to the type of aircraft (single-aisle/twin-aisle), gasper (open/closed), and heating (on/off). It shows a wider distribution of risks in the single-aisle aircraft compared with the twin-aisle aircraft (see Table S3 for the corresponding values). The categorical, as well as the smoothed fixed, effects were all highly significant ($p<2\times10^{-16}$). Generally, risks were reduced 3.7 times when the index passenger wore a mask; the overall effect was highly significant. Temperature and relative humidity also significantly affected risks. Generally, risks increased with increasing temperature (by approximately one order of magnitude from the temperature from 20°C to 26°C) and increasing humidity (by two to three orders of magnitude for relative humidity from 10% to 40%) (Figure 3). The splines in Figure 3 also show an initial faster decline of risk with increasing distance from the index passenger. In the single-aisle aircraft, the smooth effect of angle suggests that the net transport of aerosol particles was more backwards and to the left, whereas in the twin-aisle aircraft, this directional effect was less (Figure S4 shows the computed fractions, doses, and risks from the measurements). During taxi conditions, the overall effect of opening gaspers was an increase in risks by a factor of 1.5, and the overall effect of heating the blankets that were covering the passengers to mimic body heat decreased risks by a factor of 1.7 (Table 3).

Figure 4 groups the mean and 95th percentiles of the risk of contracting COVID-19 per aircraft according to flight conditions, virus load, flight duration, and comparison between estimates from measurements and CFD simulations. (Table S4 lists the mean and 95th percentiles of the risk of contracting COVID-19.)

Risk calculations for the two single-aisle aircraft studied showed that on average between 1.3×10^{-3} (measurements) and 1.1×10^{-3} (simulations) passengers will become ill (top left panel in Figure 4). For the twin-aisle aircraft, this probability ranged from 1 in 110 (measurements) to 1 in 230 (simulations). The risk

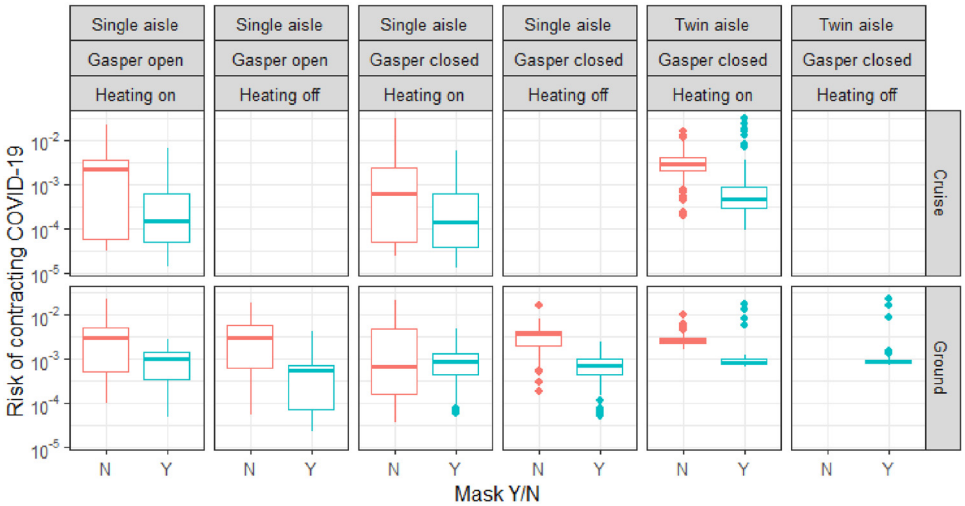

Figure 2. Box plots of the distribution of risk of contracting COVID-19 (P_{ill}) among exposed passengers in the seven rows around the index passenger. Risks are derived from the measured aerosol dispersion using Monte Carlo simulation over continuous exposure factors but distinguishing binary factors: type of aircraft (single-aisle/twin-aisle), gasper (open/closed), heating (on/off), flight conditions (cruise/taxi), and mask (Y/N). The middle line represents the median, boxes encompass the quartiles, and the whiskers represent the minimum–maximum interval. See Table S3 for risk values. Exposure time = 1 h. ©NLR & RIVM. Note: N, no; Y, yes.

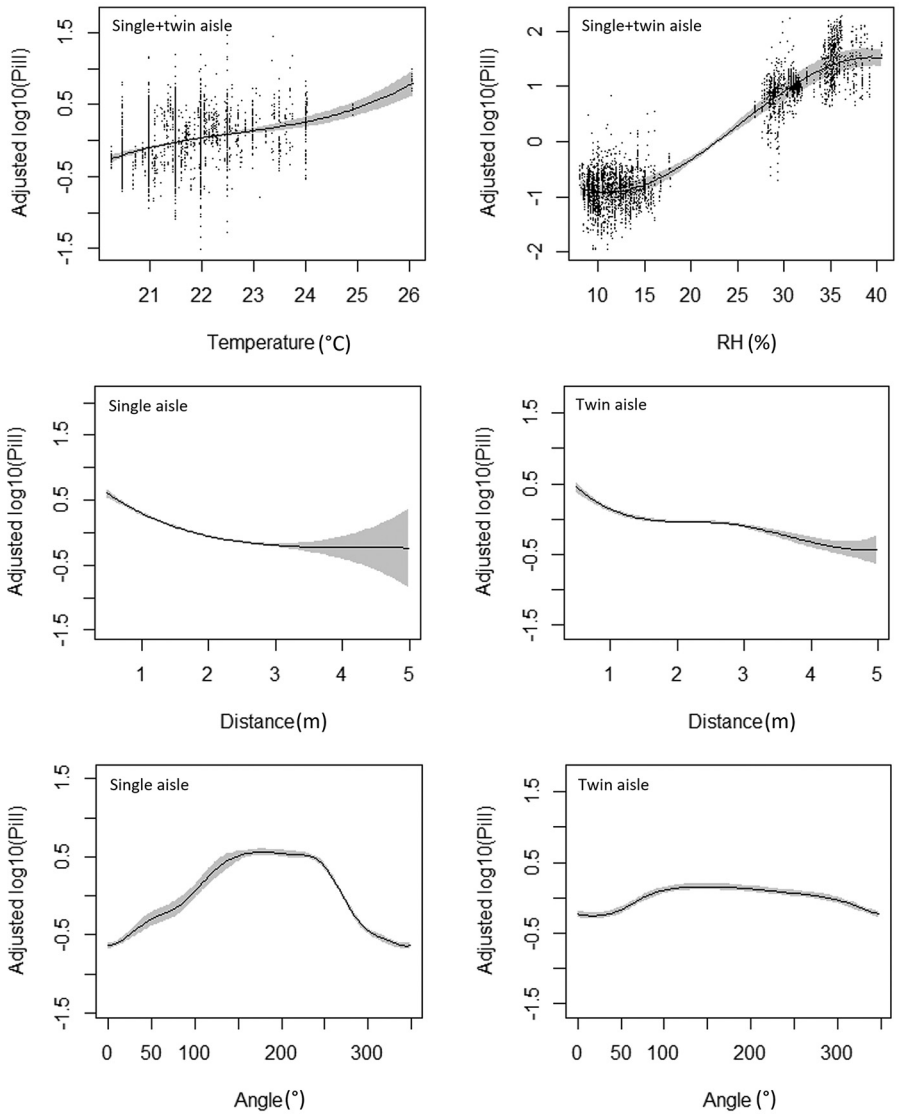

Figure 3. Splines plots (smooth effects) on risk of contracting COVID-19 (P_{ill}) of temperature, relative humidity (RH), distance from the index passenger, and the angle relative to the index passenger (0° is toward the front, 90° is to the right). The adjusted $\log_{10} p_{ill}$ is a relative measure: A value of 0 implies no effect, +1 implies 10 times higher, and −1 implies 10 times lower P_{ill}. The gray area around the spline represents the confidence interval of the spline. ©NLR & RIVM.

was highest for the twin-aisle aircraft mainly owing to the longer typical flight duration of this aircraft.

In the case of a super shedder as an index passenger (middle row panels in Figure 4), risk of SARS-CoV-2 transmission was estimated to be 6.3–7.6 times higher than in the case of an average shedder (top row panels). The estimated mean probability was that 8.3×10^{-3} up to 6.3×10^{-2} passengers will be at risk of COVID-19 illness.

Transmission risk increased as the dose increased proportionally with flight duration (compare left and right panels columns in Figure 4). The mean individual risk of contracting COVID-19 on board the single-aisle aircraft performing a longer flight was found to lie between $\sim 2.4 \times 10^{-3}$ and 2.9×10^{-3} (between 1.9×10^{-2} and 2.1×10^{-2} in case of a super shedder). For a longer twin-aisle flight, the mean individual risk varied from 5.2×10^{-3} to 1.1×10^{-2}, increasing to values between 4.0×10^{-2} and 7.7×10^{-2} when a super shedder index passenger was on board.

Per-hour flight duration risk was found to be between 3.4×10^{-4} and 1.3×10^{-3} for the single-aisle and between 7.1×10^{-4} and 1.3×10^{-3} for the twin-aisle aircraft for the average shedder and assuming mask wearing for the entire hour.

During taxiing, the mean individual risk of contracting COVID-19 for passengers varied with taxi duration (bottom panels row Figure 4). For typical taxi times, the mean risk on board the single-aisle aircraft was 3.8×10^{-4}; for longer taxi times, the value was similar: 3.2×10^{-4}. For the twin-aisle aircraft risks were 7.1×10^{-4} for a typical taxi period and 5.9×10^{-4} for a longer taxi duration.

The number of flights that was expected to result in at least one case of contracting COVID-19 was also calculated. For the most relevant scenarios, both the expected number of cases and the expected number of flights to result in (at least) one case are given in Table 4. Risks increased with increasing flight duration: 2–23 cruise flights of typical duration and 2–10 flights of longer duration resulted in at least 1 case of COVID-19 due to on board aerosol transmission by one average shedder and in the case of one super shedder, at least 1 case in 1–3 flights of typical duration cruise and 1 flight of longer duration.

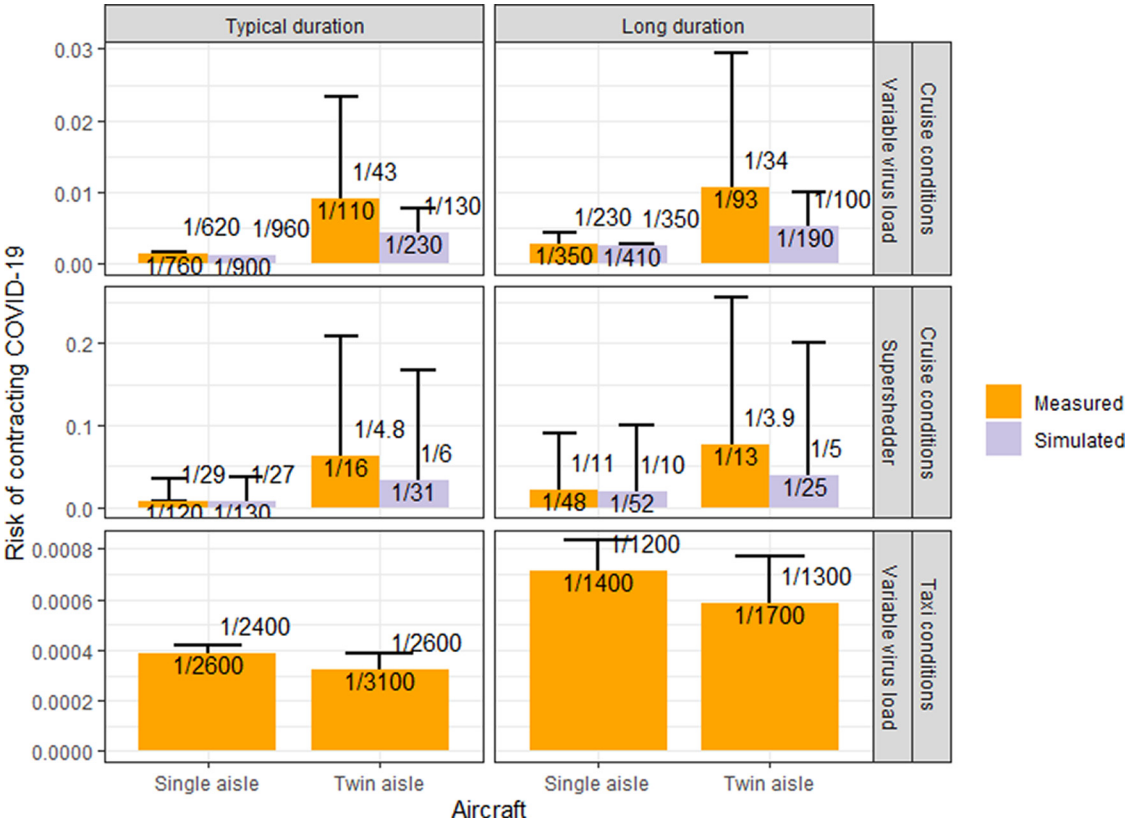

Figure 4. Bar chart of mean risk (bar) and 95th percentile (whisker) of contracting COVID-19 (P_{ill}) per aircraft grouped according to flight conditions, virus load, flight duration, and comparison between estimates from measurements and simulations. Typical cruise flight duration was 0.9 h and 1.4 h for the two single-aisle aircraft, and 8.7 h for the twin-aisle aircraft. The long (95th percentile) cruise flight duration was 2.5 h and 3.6 h for the two single-aisle aircraft, and 11.1 h for the twin-aisle aircraft. See Table S4 for the corresponding values. ©NLR & RIVM.

Discussion

The overall goal of this study was to estimate the probabilities of becoming ill with COVID-19 under various scenarios, that is, symptomatic infection. To that aim, it was assumed that the dose–response relation for the risk of illness due to exposure to coronavirus 229E applied to SARS-CoV-2, which is a precautious assumption recommended by Haas.[30] Such a precautious approach is justified considering the complexity of existing variants of the virus and vaccination status. The estimated effects of mask wearing, type of aircraft, and air conditions in the aircraft on risk changes will, nevertheless, be valid. The probability of becoming infected with the virus is higher, given that asymptomatic infections also occur. The percentage of infections that are asymptomatic were estimated at 40.5% [95% confidence interval (CI): 33.5%, 47.5%] and at 35.1% (95% CI: 30.7%, 39.9%).[40] The percentage of infections that are asymptomatic can vary with virus variant, immune status of the exposed population, and age. For example, Sah et al.[41] estimated that 19.7% of infections in elderly are asymptomatic, compared with 46.7% in children.

Variation in estimated risks (for contracting COVID-19 as a result of aerosol transmission of SARS-CoV-2) between aircraft may stem from differences in indoor aircraft conditions that lead

Table 4. Expected number of cases per flight and expected number of flights resulting in at least one case of contracting COVID-19.

	Typical cruise flight duration[a]				Long cruise flight duration[b]			
	Variable virus load		Super shedder		Variable virus load		Super shedder	
	Measured	Simulated	Measured	Simulated	Measured	Simulated	Measured	Simulated
Expected number of cases per flight								
Single-aisle[c]	0.053	0.044	0.33	0.31	0.11	0.10	0.83	0.77
Twin-aisle[d]	0.55	0.27	3.8	2.0	0.55	0.27	4.7	2.4
Expected number of flights to result in at least 1 case								
Single-aisle	19	23	3	3	9	10	1	1
Twin-aisle	2	4	1	1	2	3	1	1

Note: Expected number of cases per flight calculated by multiplying the number of passengers per flight with the mean risk of contracting COVID-16 (Figure 4; Table S4). The reciprocal value is the expected number of flights to result in at least 1 case.
[a]Typical cruise flight duration was 0.9 h and 1.4 h for the two single-aisle aircraft, and 8.7 h for the twin-aisle aircraft.
[b]Long (95th percentile) cruise flight duration was 2.5 h and 3.6 h for the two single-aisle aircraft, and 11.1 h for the twin-aisle aircraft.
[c]180 passengers.
[d]280 passengers.

to differences in aerosol transport and exposure, as well as from differences in flight duration. The latter may well be the largest contributor to the interaircraft variation. Considering the risks per hour of flight, the maximum difference between aircraft was approximately a factor of 4. Fractions of transferred aerosol particles determined for two other aircraft by Kinahan et al.,[42] namely at least 0.0046 adjacent the index passenger and 0.0002–0.0003 at the other seats, were similar to those determined in the present study. Conditions that govern differences in transmission between aircraft may therefore be limited. According to the simple sensitivity analysis, overall, the variability in aerosol transfer between aircraft is much lower than, for example, variability in virus load observed in the sputum of contagious persons or the variability in aerosol emission volume of an index passenger during breathing. The impact on the variability of the estimated risk of these latter factors may be several orders of magnitude.

Under low air humidity, risks increased with humidity. Other factors underlying the differences in conditions in the aircraft under cruise and ground conditions may possibly play a role. Recently, Verheyen and Bourouiba[43] suggested that 40%–60% relative humidity resulted in fewer deaths compared with <40% or >60% relative humidity, indicating there could be a mid-range protective effect.

The QMRA was based on simplified assumptions of a size-independent particle removal efficiency of aerosol particles of 70% by mask wearing by the source and receiver combined.[38] Mask wearing by an index passenger will also affect the distance over which particles are emitted during speech or breathing. Studies on filter efficiency of masks indicate a large variability with type of mask and measurement setup. Although overall there seems to be some indication that mask filter efficiency is dependent on particle size, the available studies do not allow the derivation of a universally valid filter characteristic function. In addition, the heterogeneity of the study methods leads to results that are difficult to compare or combine. Therefore, in this work, the QMRA was based on simplified assumptions of a size-independent particle removal efficiency of aerosol particles of 70% by mask wearing by the source and receiver combined, which was considered a plausible, somewhat pessimistic assumption of mask filter efficiency. According to the statistical analysis of the measurements, risks were generally reduced when the source wore a mask: The overall effect, independent of the type of aircraft, was highly significant ($p < 2 \times 10^{-16}$) and amounted to a risk reduction of 3.7 times (73% reduction; Table 3). This indicates a similar effect as reported by Cheng et al.[38] and may well be related to the low relative humidity of 10% during cruise conditions. Nevertheless, to what extent the measurement setup was representative of mask wearing by a human index passenger remains uncertain.

The risks of contracting COVID-19 as determined in this study are in the range of the attack rates (0%–8.2%) as found in a systematic review of SARS-CoV-2 transmission in aircraft travel.[10] Including both symptomatic and asymptomatic secondary cases, Khanh et al.[7] described a 10-h flight after which 12 of the 20 business class passengers tested positive. In the economy class, at least 2 of the other 180 passengers became positive, as well as one crew member. An attack rate of 62% in the business class area was inferred. This was much higher than in the QMRA presented in this work. Seating proximity was strongly associated with increased risk. For the whole aircraft, the attack rate was in line with this study. It should be noted that risks evaluated by Khanh et al.[7] most likely stemmed from transmission via both ballistic droplets and aerosol transmission.

Murphy et al.[12] described a 7.5-h flight to Ireland with a seat occupancy of 17% (49/283 seats) and 12 crew members. The inferred attack rate for this flight was 12/48, which is higher than the highest predicted mean transmission risks from aerosol transmission in the present study. At least 4 of the flight cases were not seated next to any other positive case, had no contact in the transit lounge, wore face masks in-flight and would not be deemed close contacts under current guidance from the European Centre for Disease Prevention and Control, rendering aerosol transmission a plausible route. Findings were confirmed by phylogeny of virus variants.

Bae et al.[13] researched virus transmission by 6 asymptomatic passengers on a 11-h evacuation flight carrying 310 passengers from Milan, Italy, to South Korea. This flight resulted in one secondary case. Overall, one symptomatic infection originating from 1 of 6 asymptomatic sources yields a 0.2% transmission probability similar to the risk of transmission during typical flight durations (8.3×10^{-4} to 8.3×10^{-3}) as estimated in the present study.

Toyokawa[11] found in their epidemiological analysis of SARS-CoV-2 transmission during a 2-h domestic flight in Japan, March 2020, that risk factors for infection included not using a face mask [adjusted odds ratio (aOR) = 7.29 (95% CI: 1.86, 28.6)], partial face mask use [aOR = 3.0 (95% CI: 0.83, 10.8)], and being seated within two rows from the index passenger [aOR = 7.47 (95% CI: 2.06, 27.2)]. The index passenger in this case was not wearing a mask, these effects were thus found for the exposed passengers, but they are in the same order of magnitude as the effect of mask wearing by the source as found in the present study.

To provide some perspective on this risk analysis, the results can be compared with studies on transmission risks in indoor settings other than aviation. For example, Moon and Ryu[44] found that transmission risks of SARS-CoV-2 were highest in residential spaces [combined relative risk (RR) = 8.30 (95% CI: 3.30, 20.90)] and airplanes [combined RR = 7.30 (95% CI: 1.15, 46.20)]. For high-speed train passengers, Hu et al.[45] found that the attack rate [0%–10.3%, with a mean of 0.32% (3.2×10^{-3})] was similar to the transmission risk estimated in the present study for the typical flight scenario and conditions. On the other hand, several cases of very high attack rates in buses and restaurants have been described. For example, Luo et al.[46] reported an attack rate of 15% or 1.4×10^{-1} for a bus passenger taking two bus trips. And Lu et al.[47] described a case study of a very high attack rate in a restaurant outbreak, where 10 of 83 (1.3×10^{-1}) customers became ill with COVID-19. This is anecdotal evidence only, but such high attack rates are higher than the estimated transmission risks in the present study.

Particle transport in airplanes has been studied both experimentally and in model simulations.,[42,48–50] Overall, these studies demonstrate particle transport is highly localized around the index location. Dispersion was found to mostly (although not exclusively) take place on the index side of the aisle, within the row where the index passenger was seated. Some longitudinal transport was observed, but this was generally much lower than the transversal (within row) transport. The results of these studies underpin the findings in our work that risks of contracting COVID-19 due to aerosol transmission in aircraft are highly heterogeneously distributed, being concentrated around the index passenger and falling off with distance (see, e.g., Figure S4).

Estimates on the likelihood of one index passenger boarding an aircraft are hard to validate, but an upper limit of 5% of the prevalence in June 2021 in the Netherlands would indicate <30/100,000 passengers. Depending on the number of passengers per aircraft (100–300), every 11–33 flights could carry an index passenger of which <3% of these could be a super shedder. Complying with all (nonpharmaceutical) mitigation strategies in place, such as good hygiene and mask wearing, will decrease the transmission, although some risk of contracting COVID-19 will remain.

In both physical measurements and computational simulation, assumptions were taken, however on different characteristics. Physical measurements and computation simulation together provide the rigor of evidence (below one order of magnitude) for risk-based decision-making. The measurements can be taken as the basis for this risk assessment and the agreement between measurements and simulations provide a means of developing more generic methods to assess risks for a variety of scenarios.

One can assume that air travel plays a role in the import and export of new variants of SARS-CoV-2 over the world. Even though variability among variants may result in differences in transmissibility and infectivity, differences between variants were outside the scope of this study.

This work combines the methods of QMRA with CFD modeling and experimental dispersion measurements. QMRA accounts quantitatively for all risk factors and provides explicit insight in their relative impact. The use of both CFD simulation and experimental measurements increases the robustness of the findings. The method can, in principle, be extended to evaluate other conditions—such as different risk-mitigation scenarios, the impact of vaccination on risk, or the risk from different virus variants—whenever quantitative information on risk factors for these situations becomes available. The present study is limited to the extent that only risks due to aerogenic transmission during flight and taxiing were considered. These risks constitute only a part of the total risks from air travel that include transmission from other routes, such as fomite and large droplet exposure, and travel phases, such as check-in and boarding. It is not known at this point whether the risks considered in this work actually constitute the largest transmission risk during air travel.

Conclusions

For a typical cruise flight (ranging between 0.9 h for the single-aisle aircraft and 8.7 h for the twin-aisle aircraft), mean risk of contracting COVID-19 owing to inhalation of aerosolized SARS-CoV-2 particles was estimated to be in the range of 8.3×10^{-4} to 8.3×10^{-3} among the passengers seated in the seven rows around the index passenger. In the case of a passenger who sheds an extraordinary amount of infectious aerosol particles (a so-called super shedder), and during a long flight in a twin-aisle aircraft, mean risks increased up to 7.7×10^{-2}. These findings were found to be in line with other model and measurement studies on in-flight risk of contracting COVID-19 as a result of inhalation of virus-bearing aerosol particles. Risks assessed in other studies varied between 1.6×10^{-3} and 4.4×10^{-3} for modest or mild emission by an index passenger (compared with 1.3×10^{-3} to 9.1×10^{-3} in the present study), to around 2.9×10^{-2} for a high emission index passenger (compared with 2.7×10^{-3} to 6.3×10^{-2} for the super shedder scenarios in the present work). Risks determined in this work (1.3×10^{-3} to 9.1×10^{-3}) for typical flight conditions were similar to attack rates observed in a study on SARS-CoV-2 transmission on board high-speed trains (3.3×10^{-3}). Targeted studies on very high attack rates in buses and restaurants, on the other hand, indicated risks as high as 1.3×10^{-1} to 5.0×10^{-1}, that is, significantly higher than this study estimated for the scenario in which a super shedder boarded the aircraft (2.1×10^{-2} to 7.7×10^{-2}).

The expected number of cruise flights that resulted in at least 1 case of COVID-19 due to aerosol transmission from a regular virus shedding index passenger was estimated to range from 2 to 23 cruise flights with durations typical for the aircraft types used in this study. In case of longer-duration cruise flights, the expected number of flights ranged from 2 to 10. The expected number of cruise flights that resulted in at least 1 case of aerosol transmission from a super shedder index passenger was estimated to range from 1 to 3 flights (typical cruise) and 1 flight (long cruise).

From this study, it can be concluded that the risk of contracting COVID-19 by aerosol transmission in an aircraft cabin is low, but that it will not be zero. Testing before boarding may help reduce the chance of a (super)shedder boarding an aircraft and mask use further reduces aerosol transmission in the aircraft cabin.

Acknowledgments

The German Aerospace Centre (DLR) and the medical equipment company Medspray provided practical support with the measurements and subsequent analysis.

The Dutch Ministry of Infrastructure and Water Management tasked the Royal Netherlands Aerospace Centre and National Institute for Public Health and the Environment in July 2020 to conduct a literature review and scientifically assess the risk of contracting COVID-19 due to aerosol transmission of SARS-CoV-2 in aircraft cabins during realistic flight operations (award ID0EBPCI36553, to J.F.S.).

References

1. ECDC (European Centre for Disease Prevention and Control). 2020. COVID-19 Aviation Health Safety Protocol: operational guidelines for the management of air passengers and aviation personnel in relation to the COVID-19 pandemic. https://www.ecdc.europa.eu/en/publications-data/covid-19-aviation-health-safety-protocol [accessed 7 November 2022].
2. Okada P, Buathong R, Phuygun S, Thanadachakul T, Parnmen S, Wongboot W, et al. 2020. Early transmission patterns of coronavirus disease 2019 (COVID-19) in travellers from Wuhan to Thailand, January 2020. Euro Surveill 25(8):2000097, PMID: 32127124, https://doi.org/10.2807/1560-7917.ES.2020.25.8.2000097.
3. Kucharski AJ, Russell TW, Diamond C, Liu Y, Edmunds J, Funk S, et al. 2020. Early dynamics of transmission and control of COVID-19: a mathematical modelling study. Lancet Infect Dis 20(5):553–558, PMID: 32171059, https://doi.org/10.1016/S1473-3099(20)30144-4.
4. Olsen SJ, Chang HL, Cheung TYY, Tang AFY, Fisk TL, Ooi SPL, et al. 2003. Transmission of the severe acute respiratory syndrome on aircraft. N Engl J Med 349(25):2416–2422, PMID: 14681507, https://doi.org/10.1056/NEJMoa031349.
5. Baker MG, Thornley CN, Mills C, Roberts S, Perera S, Peters J, et al. 2010. Transmission of pandemic A/H1N1 2009 influenza on passenger aircraft: retrospective cohort study. BMJ 340:c2424, PMID: 20495017, https://doi.org/10.1136/bmj.c2424.
6. Yang N, Shen Y, Shi C, Ma AHY, Zhang X, Jian X, et al. 2020. In-flight transmission cluster of COVID-19: a retrospective case series. Infect Dis (Lond) 52(12):891–901, PMID: 32735163, https://doi.org/10.1080/23744235.2020.1800814.
7. Khanh NC, Thai PQ, Quach HL, Thi NAH, Dinh PC, Duong TN, et al. 2020. Transmission of SARS-CoV 2 during long-haul flight. Emerg Infect Dis 26(11):2617–2624, PMID: 32946369, https://doi.org/10.3201/eid2611.203299.
8. Speake H, Phillips A, Chong T, Sikazwe C, Levy A, Lang J, et al. 2020. Flight-associated transmission of severe acute respiratory syndrome coronavirus 2 corroborated by whole-genome sequencing. Emerg Infect Dis 26(12):2872–2880, PMID: 32990563, https://doi.org/10.3201/eid2612.203910.
9. Swadi T, Geoghegan JL, Devine T, McElnay C, Sherwood J, Shoemack P, et al. 2021. Genomic evidence of in-flight transmission of SARS-CoV-2 despite predeparture testing. Emerg Infect Dis 27(3):687–693, PMID: 33400642, https://doi.org/10.3201/eid2703.204714.
10. Rosca EC, Heneghan C, Spencer EA, Brassey J, Plüddemann A, Onakpoya IJ, et al. 2021. Transmission of SARS-CoV-2 associated with aircraft travel: a systematic review. J Travel Med 28(7):taab133, PMID: 34480171, https://doi.org/10.1093/jtm/taab133.
11. Toyokawa T, Shimada T, Hayamizu T, Sekizuka T, Zukeyama Y, Yasuda M, et al. 2022. Transmission of SARS-CoV-2 during a 2-h domestic flight to Okinawa, Japan, March 2020. Influenza Other Respir Viruses 16(1):63–71, PMID: 34605181, https://doi.org/10.1111/irv.12913.
12. Murphy N, Boland M, Bambury N, Fitzgerald M, Comerford L, Dever N, et al. 2020. A large national outbreak of COVID-19 linked to air travel, Ireland, summer 2020. Euro Surveill 25(42):2001624, PMID: 33094715, https://doi.org/10.2807/1560-7917.ES.2020.25.42.2001624.
13. Bae SH, Shin H, Koo HY, Lee SW, Yang JM, Yon DK. 2020. Asymptomatic transmission of SARS-CoV-2 on evacuation flight. Emerg Infect Dis 26(11):2705–2708, PMID: 32822289, https://doi.org/10.3201/eid2611.203353.

14. Haas CN. 2020. Quantitative microbial risk assessment and molecular biology: paths to integration. Environ Sci Technol 54(14):8539–8546, PMID: 32539352, https://doi.org/10.1021/acs.est.0c00664.
15. Zaneti RN, Girardi V, Spilki FR, Mena K, Westphalen APC, da Costa Colares ER, et al. 2021. Quantitative microbial risk assessment of SARS-CoV-2 for workers in wastewater treatment plants. Sci Total Environ 754:142163, PMID: 32911141, https://doi.org/10.1016/j.scitotenv.2020.142163.
16. Shi KW, Huang YH, Quon H, Ou-Yang ZL, Wang C, Jiang SC. 2021. Quantifying the risk of indoor drainage system in multi-unit apartment building as a transmission route of SARS-CoV-2. Sci Total Environ 762:143056, PMID: 33268249, https://doi.org/10.1016/j.scitotenv.2020.143056.
17. NLR (Netherlands Aerospace Centre), RIVM (National Institute for Public Health and the Environment). 2021. *CORSICA final report: Quantitative Microbial Risk Assessment for aerosol transmission of SARS-CoV-2 in aircraft cabins based on measurements and simulations*. NLR-CR-2021-232. Amsterdam, the Netherlands: Royal Netherlands Aerospace Centre.
18. Law CC. 2019. *A Flight Attendant's Essential Guide: From Passenger Relations to Challenging Situations*. Irvine, CA: Brown Walker Press.
19. Colbeck I. 1998. *Physical and Chemical Properties of Aerosols*. Dordrecht, the Netherlands: Springer Dordrecht.
20. Liu L, Wei J, Li Y, Ooi A. 2017. Evaporation and dispersion of respiratory droplets from coughing. Indoor Air 27(1):179–190, PMID: 26945674, https://doi.org/10.1111/ina.12297.
21. Fabian P, Brain J, Houseman EA, Gern J, Milton DK. 2011. Origin of exhaled breath particles from healthy and human rhinovirus-infected subjects. J Aerosol Med Pulm Drug Deliv 24(3):137–147, PMID: 21361786, https://doi.org/10.1089/jamp.2010.0815.
22. Asadi S, Wexler AS, Cappa CD, Barreda S, Bouvier NM, Ristenpart WD, et al. 2019. Aerosol emission and superemission during human speech increase with voice loudness. Sci Rep 9(1):2348, PMID: 30787335, https://doi.org/10.1038/s41598-019-38808-z.
23. Boussinesq J. 1897. *Théorie de l'écoulement tourbillonnant et tumultueux des liquides dans les lits rectilignes a grande section*. Paris, France: Gauthier-Villars et fils.
24. OpenFOAM. 2020. OpenFoam v2006. https://www.openfoam.com [accessed 7 November 2022].
25. Tanabe SI, Kobayashi K, Nakano J, Ozeki Y, Konishi M. 2002. Evaluation of thermal comfort using combined multi-node thermoregulation (65MN) and radiation models and computational fluid dynamics (CFD). Energy Build 34(6):637–646, https://doi.org/10.1016/S0378-7788(02)00014-2.
26. Gupta JK, Lin CH, Chen Q. 2011. Transport of expiratory droplets in an aircraft cabin. Indoor Air 21(1):3–11, PMID: 21208287, https://doi.org/10.1111/j.1600-0668.2010.00676.x.
27. Davis AC, Menard DJ, Clark AD, Cummins JJ, Olson NA. 2021. Comparison of cough particle exposure for indoor commercial and aircraft cabin spaces. medRxiv. Preprint posted online March 26, 2021, https://doi.org/10.1101/2021.03.24.21254275.
28. Zee M, Davis AC, Clark AD, Wu T, Jones SP, Waite LL, et al. 2021. Computational fluid dynamics modeling of cough transport in an aircraft cabin. Sci Rep 11(1):23329, PMID: 34857807, https://doi.org/10.1038/s41598-021-02663-8.
29. Schijven J, Vermeulen LC, Swart A, Meijer A, Duizer E, de Roda Husman AM. 2021. Quantitative microbial risk assessment for airborne transmission of SARS-CoV-2 via breathing, speaking, singing, coughing, and sneezing. Environ Health Perspect 129(4):47002, PMID: 33793301, https://doi.org/10.1289/EHP7886.
30. Haas CN. 2020. Action levels for SARS-CoV-2 in air: preliminary approach. https://files.osf.io/v1/resources/erntm/providers/osfstorage/5f371de025e5dc00c4c9558f?action=download&direct&version=1 [accessed 7 November 2022].
31. Popa A, Genger JW, Nicholson MD, Penz T, Schmid D, Aberle SW, et al. 2020. Genomic epidemiology of superspreading events in Austria reveals mutational dynamics and transmission properties of SARS-CoV-2. Sci Transl Med 12(573):eabe2555, PMID: 33229462, https://doi.org/10.1126/scitranslmed.abe2555.
32. Wolfram Research, Inc. 2021. *Mathematica*. Version 12.3 ed. Champaign, IL: Wolfram Research, Inc.
33. Chu DK, Akl EA, Duda S, Solo K, Yaacoub S, Schünemann HJ, et al. 2020. Physical distancing, face masks, and eye protection to prevent person-to-person transmission of SARS-CoV-2 and COVID-19: a systematic review and meta-analysis. Lancet 395(10242):1973–1987, PMID: 32497510, https://doi.org/10.1016/S0140-6736(20)31142-9.
34. Esposito S, Principi N, Leung CC, Migliori GB. 2020. Universal use of face masks for success against COVID-19: evidence and implications for prevention policies. Eur Respir J 55(6):2001260, PMID: 32350103, https://doi.org/10.1183/13993003.01260-2020.
35. Fischer EP, Fischer MC, Grass D, Henrion I, Warren WS, Westman E. 2020. Low-cost measurement of face mask efficacy for filtering expelled droplets during speech. Sci Adv 6(36):eabd3083, PMID: 32917603, https://doi.org/10.1126/sciadv.abd3083.
36. Howard J, Huang A, Li Z, Tufekci Z, Zdimal V, van der Westhuizen HM, et al. 2020. Face masks against COVID-19: an evidence review. Preprints. Preprint posted online April 12, 2020, https://doi.org/10.20944/preprints202004.0203.v1.
37. Leung NHL, Chu DKW, Shiu EYC, Chan KH, McDevitt JJ, Hau BJP, et al. 2020. Respiratory virus shedding in exhaled breath and efficacy of face masks. Nat Med 26(5):676–680, PMID: 32371934, https://doi.org/10.1038/s41591-020-0843-2.
38. Cheng VCC, Wong SC, Chan VWM, So SYC, Chen JHK, Yip CCY, et al. 2020. Air and environmental sampling for SARS-CoV-2 around hospitalized patients with coronavirus disease 2019 (COVID-19). Infect Control Hosp Epidemiol 41(11):1258–1265, PMID: 32507114, https://doi.org/10.1017/ice.2020.282.
39. Wood SN. 2006. *Generalized Additive Models: An Introduction with R*. Boca Raton, FL: Chapman and Hall/CRC Press.
40. Ma Q, Liu J, Liu Q, Kang L, Liu R, Jing W, et al. 2021. Global percentage of asymptomatic SARS-CoV-2 infections among the tested population and individuals with confirmed COVID-19 diagnosis: a systematic review and meta-analysis. JAMA Netw Open 4(12):e2137257, PMID: 34905008, https://doi.org/10.1001/jamanetworkopen.2021.37257.
41. Sah P, Fitzpatrick MC, Zimmer CF, Abdollahi E, Juden-Kelly L, Moghadas SM, et al. 2021. Asymptomatic SARS-CoV-2 infection: a systematic review and meta-analysis. Proc Natl Acad Sci USA 118(34):e2109229118, PMID: 34376550, https://doi.org/10.1073/pnas.2109229118.
42. Kinahan SM, Silcott DB, Silcott BE, Silcott RM, Silcott PJ, Silcott BJ, et al. 2021. Aerosol tracer testing in Boeing 767 and 777 aircraft to simulate exposure potential of infectious aerosol such as SARS-CoV-2. PLoS One 16(12):e0246916, PMID: 34851965, https://doi.org/10.1371/journal.pone.0246916.
43. Verheyen CA, Bourouiba L. 2022. Associations between indoor relative humidity and global COVID-19 outcomes. J R Soc Interface 19(196):20210865, PMID: 36382379, https://doi.org/10.1098/rsif.2021.0865.
44. Moon J, Ryu BH. 2021. Transmission risks of respiratory infectious diseases in various confined spaces: a meta-analysis for future pandemics. Environ Res 202:111679, PMID: 34265349, https://doi.org/10.1016/j.envres.2021.111679.
45. Hu M, Lin H, Wang J, Xu C, Tatem AJ, Meng B, et al. 2021. Risk of coronavirus disease 2019 transmission in train passengers: an epidemiological and modeling study. Clin Infect Dis 72(4):604–610, PMID: 32726405, https://doi.org/10.1093/cid/ciaa1057.
46. Luo K, Lei Z, Hai Z, Xiao S, Rui J, Yang H, et al. 2020. Transmission of SARS-CoV-2 in public transportation vehicles: a case study in Hunan Province, China. Open Forum Infect Dis 7(10):ofaa430, PMID: 33123609, https://doi.org/10.1093/ofid/ofaa430.
47. Lu J, Gu J, Li K, Xu C, Su W, Lai Z, et al. 2020. COVID-19 outbreak associated with air conditioning in restaurant, Guangzhou, China, 2020. Emerg Infect Dis 26(7):1628–1631, PMID: 32240078, https://doi.org/10.3201/eid2607.200764.
48. Zhang M, Yu N, Zhang Y, Zhang X, Cui Y. 2021. Numerical simulation of the novel coronavirus spread in commercial aircraft cabin. Processes 9(9):1601, https://doi.org/10.3390/pr9091601.
49. Pavlik JA, Ludden IG, Jacobson SH. 2022. SARS-CoV-2 aerosol risk models for the airplane seating assignment problem. J Air Transp Manag 99:102175, PMID: 34876782, https://doi.org/10.1016/j.jairtraman.2021.102175.
50. Li X, Zhang TT, Fan M, Liu M, Chang D, Wei ZD, et al. 2021. Experimental evaluation of particle exposure at different seats in a single-aisle aircraft cabin. Build Environ 202:108049, PMID: 34155419, https://doi.org/10.1016/j.buildenv.2021.108049.